Coherent Intramolecular Dynamics of Enzymic Reaction Loops in Small Volumes

Pedro Stange,[†] Alexander S. Mikhailov,[*,†] and Benno Hess[‡,§]

Abteilung Physikalische Chemie, Fritz-Haber-Institut der Max-Planck-Gesellschaft, Faradayweg 4-6, D-14195 Berlin (Dahlem), Germany, and Max-Planck-Institut für Molekulare Physiologie, Otto-Hahn-Strasse 11, D-44227 Dortmund, Germany

Received: July 28, 1999

The diffusive transport and mixing times of regulatory molecules in micrometer and submicrometer reaction volumes can be shorter than characteristic times of conformational transformations in single enzyme molecules. Under these conditions, synchronization of individual molecular turnover cycles takes place when a fraction of the reaction products is converted through a second chemical reaction into the substrate molecules. Using a stochastic model which explicitly describes the internal dynamics of the catalytic process, we analyze the properties of the synchronization transition and the role of statistical fluctuations in the synchronization phenomena.

1. Introduction

Complex internal dynamics of conformational transformations in single enzyme molecules is essential for their catalytic function.[1,2] Such experimental methods as time-resolved X-ray spectroscopy of protein crystals or single-molecule fluorescence microscopy[3−6] allow observation of individual enzymic turnover cycles.[7,8] Enzymic reactions in living biological cells are confined to very small spatial volumes, and this can lead to qualitative changes in the kinetics of biochemical reactions.[9,10] It has recently been suggested that classical concepts of chemical kinetics must be revised when processes inside living cells are considered.[11] New approaches are needed to take into account interactions between protein machines of the living cell and treat the cell as a whole.[12] Investigations of complete enzymic reactions in biologically relevant nanoenviroments are now possible.[13]

Experiments with the photosensitive cytochrome P-450 dependent monooxygenase system have shown[14−16] that the turnover cycles of individual enzymes can be externally synchronized by applying periodic light flashes. Another type of external synchronization has been discussed in the membrane transport system of the enzyme Na,K-ATPase using external electric fields.[17] In a series of publications we have recently found that mutual synchronization of individual turnover cycles of enzymes can take place in reactions with allosteric product activation[18−20] and allosteric product inhibition[21] in small spatial volumes. The common conclusion of these experimental and theoretical investigations is that *coherent* intramolecular dynamics may emerge as a consequence of external forcing or interactions between the molecules. This microscopic coherence in ensembles of protein macromolecules is a new property absent in macroscopic chemical kinetics.

So far the possibility of mutual synchronization of enzymic molecular turnover cycles has only been shown for the examples of reactions where allosteric regulation was involved. The aim of the present paper is to prove that a spontaneous transition to the microscopic coherent regime, characterized by synchronization of molecular turnover cycles, can as well occur in biochemical reactions which are not allosterically regulated.

As an example we consider a hypothetical enzymic reaction chain where a fraction of reaction products is converted back to the substrate and thus a closed loop is formed. We analyze the kinetics of this reaction in a small volume, where diffusional mixing and transport times of substrate and products are much shorter than the turnover time of a single catalytic cycle. Under such conditions each of the chemical reactions in the chain is coupled to others via fast diffusing substrate and product molecules. The situation differs from that described in the macroscopic chemical kinetics, since the intramolecular dynamics is then much slower than all diffusion-related processes. We find that coherent intramolecular dynamics is possible in this system and investigate statistical properties of this special kinetic regime.

In the next section a stochastic model of the investigated reaction chain is introduced. The results of numerical simulations of the microscopic reaction kinetics are presented in section 3. In section 4, the mean-field approximation for a slightly simplified model is constructed and a linear stability analysis is performed to determine synchronization boundaries in the parameter space. The Appendix presents the algorithms used in our numerical stochastic simulations.

2. Stochastic Model

Metabolic pathways in living cells consist of a large number of reactions catalyzed by enzymes. A particular reaction is embedded in such a pathway, taking product molecules of the previous reaction step and supplying the substrate for the next step. Additionally, links between different metabolic cycles can be formed through common use of some reactants. The structure of metabolic pathways and interactions between them shows a great variety. Some reaction chains, such as substrate cycles,[22] contain closed loops where a large fraction of product molecules are converted back to the substrate molecules of the same reaction.

* To whom correspondence should be addressed. E-mail: mikhailov@fhi-berlin.mpg.de.
† Fritz-Haber-Institut der Max-Planck-Gesellschaft.
‡ Max-Planck-Institut für Molekulare Physiologie.
§ Current address: Max-Planck-Institut für Medizinische Forschung, Jahnstrasse 29, D-69120 Heidelberg, Germany.

10.1021/jp992641q CCC: $19.00
Published on Web 02/03/2000

In this paper we shall consider a hypothetical reaction chain including a closed loop:

$$\begin{gathered} S + E \xrightarrow{\alpha} ES \rightarrow P + E \\ P \xrightarrow{\kappa} S, \quad P \xrightarrow{\gamma_1} C \\ A \xrightarrow{\zeta} S, \quad S \xrightarrow{\gamma} B \end{gathered} \tag{1}$$

Binding of a substrate molecule *S* initiates the catalytic turnover cycle of enzyme E during which a product molecule appears. A free product molecule P is transformed through a different chemical reaction back into a substrate molecule. Moreover, substrate and product molecules are consumed by other reactions, transforming them into molecules B and C that do not further participate in the considered set of reactions. Substrate is supplied through chemical conversion of molecules A. The concentration of these molecules A is maintained constant. The classical kinetic equations of such a reaction chain are linear and do not show any self-sustained oscillations. Note that the enzyme is not allosteric and its catalytic activity is not regulated in the considered system.

We assume that these reactions proceed in a small volume, so that the conditions of a molecular network are satisfied. These conditions are[10,18,23]

$$\tau \gg t_{\text{transit}} > t_{\text{mix}} \tag{2}$$

Here τ is the turnover time, i.e., the time needed by an enzyme molecule to transform the substrate molecule into the product and return to its initial state, where it can again bind a substrate molecule, t_{mix} is the diffusive mixing time of substrate molecules in the reaction volume, and t_{transit} is the transit time needed by a substrate molecule to reach by diffusion and bind at the binding site on the surface of an enzyme. If $t_{\text{transit}} > t_{\text{mix}}$, the initial position of a substrate molecule is already forgotten when it binds to an enzyme, and therefore it can bind with the same probability to any enzyme molecule in the reaction volume. This means that the system is perfectly mixed and the spatial coordinates of substrate molecules are irrelevant. The condition $\tau \gg t_{\text{transit}}$ implies that the transport time of molecules is much shorter than the duration of a single molecular catalytic cycle. In this case the reaction system can be viewed as a population of fast communicating dynamical elements with slow periodic dynamics.

The characteristic mixing and transit times for the substrate molecules in a reaction volume of linear size L containing N enzymes are given, respectively, by the estimates $t_{\text{mix}} = L^2/D$ and $t_{\text{transit}} = L^3/NDR$, where R is the radius of the atomic target group on the surface of the enzyme molecule, representing its binding site, and D is the diffusion constant of the substrate molecules. Therefore, the condition $t_{\text{transit}} > t_{\text{mix}}$ implies that the total number of enzyme molecules in the reaction volume is smaller than $N_{\text{cr}} = L/R$. For a micrometer reaction volume and a target group of a nanometer radius, this yields $N_{\text{cr}} = 1000$, which is about 10^{-6} M.[10]

In molecular networks the dynamical properties of each single enzyme are important. The actual intramolecular dynamics of such macromolecules is extremely complex and is not completely known. To model these intramolecular processes, large simplifications are needed. Following our previous publications[19−21] (see also ref 16), the dynamics of a single enzyme molecule during the catalytic turnover cycle is modeled below as diffusive motion along a certain reaction coordinate. The enzymic cycle also includes such stochastic events as binding and dissociation of substrate and product molecules (Figure 1).

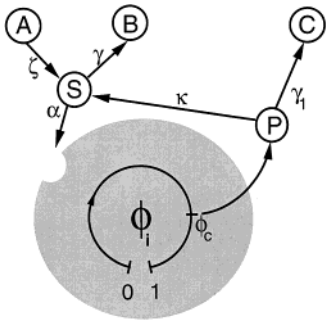

Figure 1. Schematic representation of an enzymic turnover cycle. The cycle is initiated by binding of a substrate molecule at rate α and modeled as diffusive motion along the reaction coordinate ϕ increasing from $\phi = 0$ to $\phi = 1$. At stage $\phi = \phi_c$ inside the cycle a product molecule is released that can later be converted into molecules of type C at rate γ_1 and can be converted back into substrate molecules at rate κ. The substrate molecules are permanently supplied by converting molecules of type A into substrate at rate ζ. Additionally, substrate can be converted into molecules of type B at rate γ.

It is convenient to define for each enzyme i a binary state variable u_i, such that $u_i = 0$, if the enzyme is in its free state and ready to bind a substrate molecule. The formation of an enzyme-substrate complex with rate α is then described as a transition into the state with $u_i = 1$. This transition initiates the turnover cycle, which consists of the catalytic conversion of the substrate into the product and subsequent return of the enzyme into its free state. This process is modeled as diffusional drift through an energy landscape along the reaction coordinate ϕ_i. The coordinate $\phi_i = 0$ corresponds to the beginning of the cycle. The cycle ends when $\phi_i = 1$ and the enzyme returns to its free state with $u_i = 0$. The release of the product molecule takes place at point $\phi_i = \phi_c$ inside the cycle. Thus, the point ϕ_c on the reaction coordinate separates two different processes. In the coordinate interval $0 < \phi_i < \phi_c$ the enzyme-substrate complex exists, whereas later in the interval $\phi_c < \phi_i < 1$ the enzyme undergoes conformational relaxation back to its free state. Then, it can bind again a substrate molecule to start a new cycle.

Introducing the probability distribution $p(\phi_i,t)$ over the reaction coordinate ϕ_i, we assume that this distribution satisfies the diffusion equation

$$\frac{\partial p}{\partial t} = -\upsilon \frac{\partial p}{\partial \phi_i} + \sigma \frac{\partial^2 p}{\partial \phi_i^2} \tag{3}$$

The first term in this equation describes the drift, and the second term takes into account thermal fluctuations inside the cycle. This diffusion equation is equivalent to the following stochastic Langevin equation:

$$\frac{\mathrm{d}\phi_i}{\mathrm{d}t} = \upsilon + \eta_i(t) \tag{4}$$

where υ is the drift velocity and $\eta_i(t)$ is white Gaussian noise with the correlation function

$$\langle \eta_i(t)\, \eta_j(t') \rangle = 2\sigma\delta_{ij}\delta(t-t') \tag{5}$$

The parameter σ determines the noise intensity. The velocity υ depends on the potential of the free energy profile. This profile is a specific property of the chosen type of enzymes and may generally have a very complicated shape. Today not much is

known about this property of real enzymes. In our following investigations, we assume a constant negative slope of the energy landscape, so that the drift velocity v is constant. The drift velocity is used to define two characteristic times

$$\tau_1 = \frac{\phi_c}{v} \quad \text{and} \quad \tau_0 = \frac{1}{v} \tag{6}$$

needed after the cycle initiation in the absence of fluctuations to release a product molecule and to finish the cycle, respectively.

The cycle starts at $\phi = 0$ and is finished after a certain time τ at $\phi = 1$. This is the turnover time that specifies the cycle duration. According to eq 4, the motion inside the cycle is a random process, and therefore the turnover time fluctuates from one realization of this process to another. The mean turnover time is estimated as (see ref 20)

$$\langle\tau\rangle = \frac{1}{v} - \frac{\sigma}{v^2}[1 - e^{-v/\sigma}] \tag{7}$$

and its statistical dispersion $\Delta\tau = (\langle\tau^2\rangle - \langle\tau\rangle^2)^{1/2}$ is given by (see ref 20)

$$\Delta\tau^2 = \frac{2\sigma}{v^3} - \frac{5\sigma^2}{v^4} + \frac{4\sigma}{v^3}e^{-v/\sigma} + \frac{4\sigma^2}{v^4}e^{-v/\sigma} + \frac{\sigma^2}{v^4}e^{-2v/\sigma} \tag{8}$$

The relative statistical dispersion is defined as

$$\xi = \frac{\Delta\tau}{\langle\tau\rangle} \tag{9}$$

For small noise intensities σ, the approximations $\langle\tau\rangle \approx 1/v$, $\Delta\tau \approx (2\sigma/v^3)^{1/2}$, and $\xi = (2\sigma/v)^{1/2}$ hold.

The dispersion ξ of turnover times is an important statistical property of the intramolecular dynamics that is more amenable for direct measurement than the intensity σ of the intramolecular noise. The two parameters are connected by a simple relationship (see eqs 8 and 9). When results of our numerical simulations are presented below, we typically give only the value of the dispersion ξ corresponding to a particular simulation. In all considered cases, the intramolecular noise is always relatively small and its intensity can be estimated as $\sigma = v\xi^2/2$.

The first step of the enzymic reaction 1 is the formation of an enzyme-substrate complex at rate constant α. When the enzyme passes the phase state ϕ_c, a product molecule is released and increases the number of free enzymes by one. Subsequent relaxations of the enzymic conformation brings the enzyme i back to the free state where $u_i = 0$.

The number of free products decreases at rate constant κ due to the conversion to substrate molecules. To prevent accumulation of products, we assume that the product molecules decay at rate γ_1. The "decay" is actually represented by the conversion of products into another chemical species C along the reaction pathway that do not further participate in the reaction. Typically we assume that $\kappa \leq \gamma_1 \ll \tau_0^{-1}$, so that the lifetime of free product molecules is short as compared with the turnover time.

Besides the decrease of substrate molecules at a rate constant α through formation of the enzyme-substrate complex, a second reaction at rate γ proceeds, transforming the substrate into molecules of type B which do not further participate in the reaction. The substrate is supplied through conversion of the chemical species A at a rate constant ζ.

The detailed numerical algorithm of this stochastic model is given in the Appendix.

3. Synchronization of Turnover Cycles

Now we present results of numerical investigations of the stochastic model. The total amount of enzymes is $N = 1000$ in all our simulations. As the initial condition, we assume that the enzymic states are randomly distributed over their cycle phase. Simulations of this model show, depending on the parameters α, γ_1, γ, ξ, ϕ_c, κ, and ζ, the existence of two qualitatively different types of behavior.

At small values of α and high values of the relative statistical dispersion ξ of the turnover time, the numbers of products, substrates, and free enzymes fluctuate randomly around a certain mean value. This is seen in Figure 2a, where the number $s(t)$ of substrate molecules (black) and the number $n(t)$ of free enzymes (gray) in the reaction volume are shown as functions of time. If the dispersion ξ of molecular turnover times is relatively small, the system can however exhibit rapid oscillations (spiking) in the numbers of substrates, products, and free enzymes. This behavior is displayed in Figure 2b, where again (using the same notations as in Figure 2a) the numbers of substrates and free enzymes are shown.

We see in Figure 2b that a certain phase shift between the numbers of free enzymes and substrates is present in the spiking regime. Whenever the substrate reaches its minimum number, the amount of free enzymes reaches its maximum. At different parameters the spiking frequency can be higher than in Figure 2b. Depending on the value of the parameter ϕ_c that characterizes the moment inside the cycle where a product molecule is released, spiking with a double frequency (Figure 2c, $\phi_c = 0.55$) or with a frequency 3 times higher than in Figure 2b (Figure 2d, $\phi_c = 0.36$) is found.

Periodic spiking in the number of free enzyme molecules indicates the presence of coherence in the intramolecular dynamics of individual enzyme molecules. Indeed, this implies that the moments, when the cycles of different enzymes are initiated, are strongly correlated and synchronous. The duration and other parameters of the individual molecular cycle, such as ϕ_c, play an important role in this kinetic regime by directly determining the spiking period. Spiking periods that are 2 or 3 times shorter than the turnover time indicate that the entire population of enzyme molecules breaks down into two or three coherently operating groups whose turnover cycles are shifted by half or one-third of a period. It should be stressed that, in contrast to the previously investigated systems where a similar coherent behavior was found,[20] the synchronization is not now a result of allosteric regulation of the enzymic activity.

The original model 1 can be simplified without losing its principle properties. We assume below that the decay of the product is absent ($\gamma_1 = 0$). Moreover, the rate constant κ of the back reaction is assumed to be much higher than the inverse τ_0^{-1} of the turnover time. The release of a product molecule by enzyme i at $\phi_i = \phi_c$ then leads immediately to an increase in the number of free substrate molecules by one. In this case, the number $n(t)$ of free products is negligibly small (it goes to zero for $\kappa \to \infty$) and it is enough to follow only the number $s(t)$ of substrate molecules in the reaction volume. Under these assumptions reaction 1 can be effectively written as

$$\begin{gathered} S + E \xrightarrow{\alpha} ES \to S + E \\ A \xrightarrow{\zeta} S, \quad S \xrightarrow{\gamma} B \end{gathered} \tag{10}$$

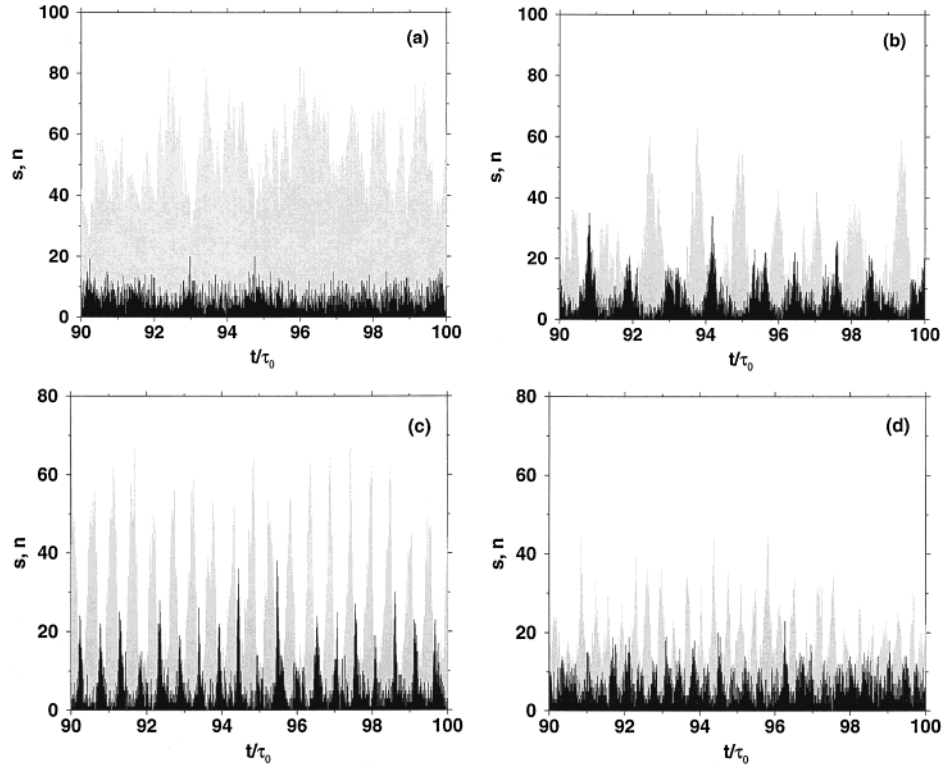

Figure 2. Time dependence of the number of substrate molecules (black) and free enzymes (gray) in the stochastic model of reaction 1 in the case of (a) no spiking at $\alpha = 3\tau_0^{-1}$, $\phi_c = 0.2$, and $\xi = 0.4$, (b) spiking with $\omega \approx 2\pi\tau_0^{-1}$ at $\alpha = 10\tau_0^{-1}$, $\phi_c = 0.2$, and $\xi = 0.15$, (c) spiking with $\omega \approx 4\pi\tau_0^{-1}$ at $\alpha = 10\tau_0^{-1}$, $\phi_c = 0.55$, and $\xi = 0.02$, and (d) spiking with $\omega \approx 6\pi\tau_0^{-1}$ at $\alpha = 10\tau_0^{-1}$, $\phi_c = 0.72$, and $\xi = 0.01$. Other parameters are $N = 1000$, $\gamma = 25\tau_0^{-1}$, $\gamma_1 = 5\tau_0^{-1}$, and $\zeta = 200\tau_0^{-1}$.

According to this scheme, substrate molecules become bound to the enzyme, spend some time in the enzyme-substrate complex, and are then released as product molecules that are instantaneously converted back to the substrate. The enzyme returns after a while to its free state and can again bind the substrate. The substrate molecules are supplied at rate ζ and decay at rate γ. The complete numerical algorithm of the simplified model is again described in the Appendix.

Results of numerical simulations of this simplified model are shown in Figure 3. We see that both spiking and random fluctuations around a certain mean value are possible, similar to what has been found in the original model (Figure 2). Figure 3a displays the time-dependent number of free enzymes (gray) and substrate molecules (black) in the spiking regime at $\phi_c = 0.2$ and $\xi = 0.02$. This spiking has a period close to the turnover time τ. By varying the parameter ϕ_c, spiking with shorter periods can also be achieved. For example, when $\phi_c = 0.55$ and $\xi = 0.02$, the spiking period is approximately $0.5\tau_0$ (Figure 3b). Our simulations have shown that spiking with even higher period is also observed in the model, but it is possible only at extremely low relative statistical dispersions ξ of the turnover time. Therefore, below we shall investigate only the spiking regimes with periods close to τ_0 and $0.5\tau_0$ which are more robust against fluctuations.

Generally, increasing the intensity σ of intramolecular noise, which determines the dispersion ξ of turnover times, leads to the breakdown of spiking and the onset of the incoherent kinetic regime, similar to that shown in Figure 2a. A more complex behavior was however found when, at small fluctuation intensity, spiking with two enzymic groups (i.e., with period $0.5\tau_0$) took place.

If we fix the parameter ϕ_c at 0.55 and begin to increase σ and, hence, the dispersion ξ, the synchronous spiking with period $0.5\tau_0$ (seen in Figure 3b) first becomes weaker and then vanishes. The appearing incoherent regime is displayed in Figure 3c for $\xi = 0.05$. However, when the statistical dispersion of turnover cycles is further increased, spiking reemerges! Now it has however a period close to the mean turnover time and thus corresponds to the presence of a single synchronous enzymic group (see Figure 3d for $\xi = 0.19$). When the dispersion ξ is increased even further, this coherent regime is also destabilized and replaced by incoherent fluctuations of individual enzymic activity.

Hence, at $\phi_c = 0.55$ three different dynamical regimes can be found. For small fluctuations we find spiking with period $0.5\tau_0$, inside an intermediate range of ξ, spiking is absent and occurs again for larger ξ with period τ_0. Thus, an increase in the intensity of the intramolecular noise can induce a transition from one kind of coherent collective molecular dynamics to another.

To quantify the strength of synchronization, we already used in our previous publications[20,21] a special order parameter. Its definition is based on the distribution

$$P(\Delta\phi) = \langle [\sum_{i,j=1,i\neq j}^{N} u_i u_j]^{-1} \sum_{i,j=1,i\neq j}^{N} u_i u_j \delta(\phi_i - \phi_j - \Delta\phi) \rangle \quad (11)$$

that specifies the probability density to find a phase difference $\Delta\phi$ between two enzymes. Since $u_i = 0$ for enzymes in the free states, the summation is performed here only over enzymes inside their turnover cycles ($u_i = 1$). Angular brackets denote time averaging over sufficiently long intervals of time to eliminate fluctuations. The coefficient with square brackets in eq 11 represents the normalization factor; $\delta(x)$ is the Dirac delta-function. When the phase states of different enzymes are not correlated, all phase differences are equally probable. Then the distribution $P(\Delta\phi)$ is flat. If, however, the synchronization of

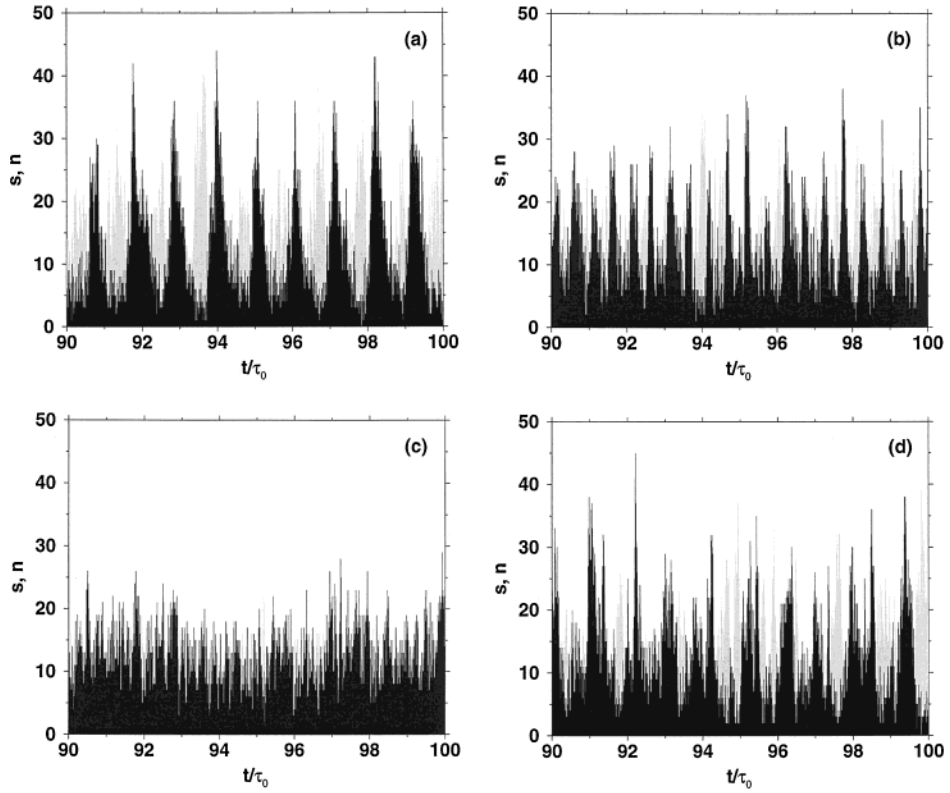

Figure 3. Time dependence of the number of substrate molecules (black) and free enzymes (gray) in the stochastic model of reaction 10 in the case of (a) spiking with $\omega \approx 2\pi\tau_0^{-1}$ at $\phi_c = 0.2$ and $\xi = 0.02$, (b) spiking with $\omega \approx 4\pi\tau_0^{-1}$ at $\phi_c = 0.55$ and $\xi = 0.02$, (c) no spiking at $\phi_c = 0.55$ and $\xi = 0.05$, and (d) spiking with $\omega \approx 2\pi\tau_0^{-1}$ at $\phi_c = 0.55$ and $\xi = 0.19$. Other parameters are $N = 1000$, $\gamma = 15\xi^{-1}$, $\zeta = 200\tau_0^{-1}$, and $\alpha = 10\tau_0^{-1}$.

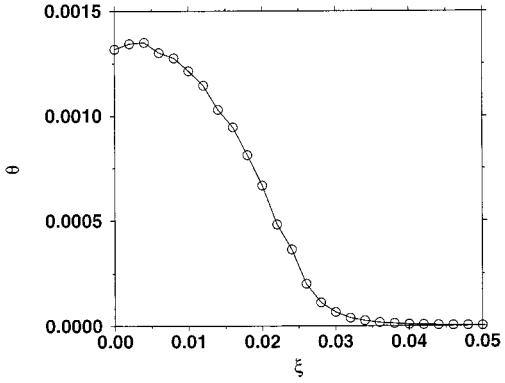

Figure 4. Dependence of the order parameter θ on the relative statistical dispersion ξ. The reaction parameters are $N = 1000$, $\alpha = 10\tau_0^{-1}$, $\gamma = 15\tau_0^{-1}$, $\zeta = 200\tau_0^{-1}$, and $\phi_c = 0.55$.

enzymic states takes place, the probability distribution $P(\Delta\phi)$ shows a maximum at $\Delta\phi = 0$.

The order parameter, characterizing the strength of synchronization, is now defined as

$$\theta = \int_{-0.5}^{0.5} (P(\Delta\phi) - 1)^2 \, d\Delta\phi \qquad (12)$$

If the correlations between the phases of different enzymes are absent, $\theta = 0$. Nonvanishing values of θ indicate the presence of synchronization.

Figure 4 shows the computed dependence of the order parameter θ on the statistical dispersion ξ of the turnover time at $\phi_c = 0.55$. The other parameters are the same as in Figure 3b−d. With increasing ξ, θ becomes very small when ξ is larger than 0.05.

Despite the fact that the order parameter θ is extremely small, visual examinations of time plots show that irregular spiking persists to much higher statistical dispersions (see, e.g., Figure 3d with $\xi = 0.19$). This indicates that the order parameter θ may be too sensitive to fluctuations, as was already noted in our previous publication.[20]

To analyze the time dependence in the number of substrate molecules, we use the autocorrelation function

$$c(t') = \frac{\langle y(t)\, y(t+t')\rangle}{\langle y^2(t)\rangle}, \quad y = s(t) - \langle s(t)\rangle \qquad (13)$$

Figure 5 displays this autocorrelation function of the time-dependent number of substrate molecules at four different values of the relative statistical dispersion ξ of the turnover time at the same reaction parameters as in Figure 4.

When the system exhibits spiking, the correlation function shows weakly damped periodic oscillations with the period close to $\tau_0/2$ (Figure 5a at $\xi = 0.02$). The amplitude of these oscillations decreases and the damping rate increases if ξ is slightly increased (Figure 5b at $\xi = 0.035$). Further increase of this control parameter leads to a more complex behavior of the correlation function. In Figure 5c at $\xi = 0.05$ the oscillations of the correlation function contain several frequencies, whereas at $\xi = 0.02$ (Figure 5d) the correlation function exhibits damped oscillations with a period close to τ_0.

Although simulations of the stochastic model given by eqs 34, 35, and 38 already provide much information about the behavior of the considered system, further analytical investigations are needed to predict the synchronization threshold and to better understand the effects of fluctuations on the synchronization behavior. Such analytical investigations are performed below.

4. Mean-field Approximation

The mean-field approximation in chemical kinetics consists of neglecting fluctuations in concentrations of reactants that are

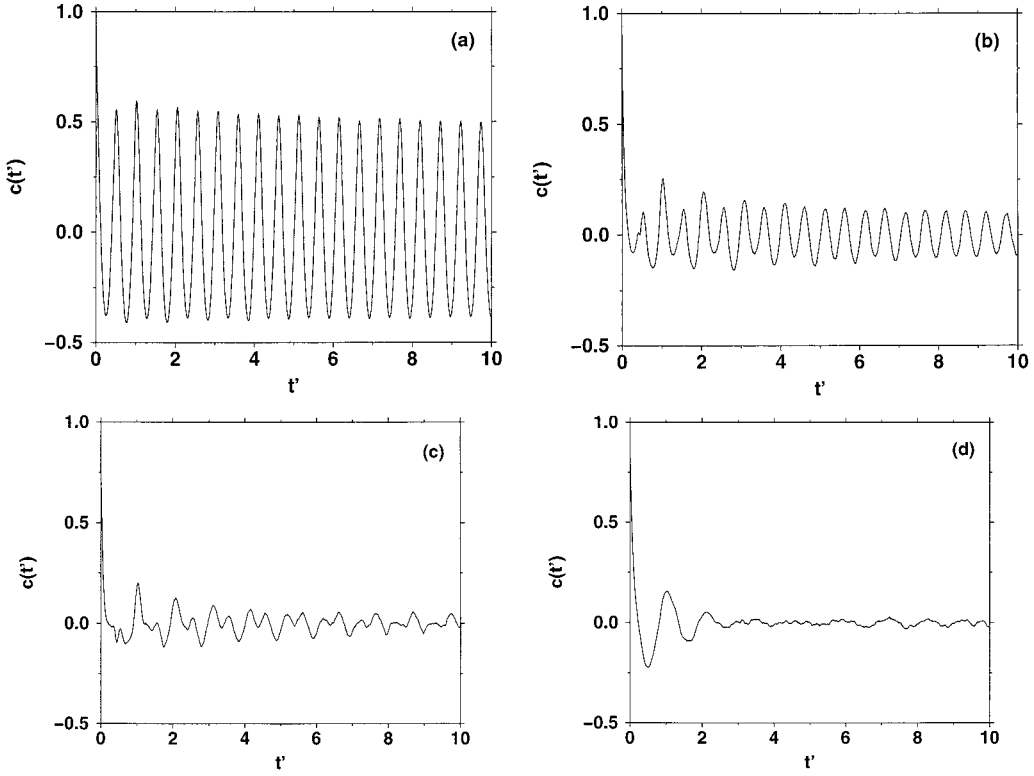

Figure 5. Correlation function $c(t')$ at (a) $\xi = 0.02$, (b) $\xi = 0.035$, (c) $\xi = 0.05$, and (d) $\xi = 0.19$. Other parameters are the same as in Figure 3.

due to the atomistic stochastic nature of reaction processes. In the limit $N \to \infty$ our system can then be completely described by the density function $\tilde{n}(\phi,t)$ such that $\tilde{n}(\phi,t)\,\Delta\phi$ gives the mean number of enzymes at time t inside the cycle in the phase states between ϕ and $\phi + \Delta\phi$. We also introduce the mean number n of free enzymes that are ready to bind the substrate. Moreover, $s(t)$ is the mean number of free substrate molecules at time t.

The evolution equation for $\tilde{n}(\phi,t)$ is

$$\frac{\partial \tilde{n}}{\partial t} = -\upsilon \frac{\partial \tilde{n}}{\partial \phi} + \sigma \frac{\partial^2 \tilde{n}}{\partial \phi^2} \tag{14}$$

Thus, evolution of the density function $\tilde{n}(\phi,t)$ represents a drift with constant velocity υ accompanied by diffusion along the reaction coordinate ϕ. The effective diffusion is caused by intramolecular fluctuations with intensity σ.

The reaction coordinate varies from $\phi = 0$ to $\phi = 1$. Additionally, there is a special point $\phi = \phi_c$ inside the cycle. It is convenient to divide the whole variation interval of the reaction coordinate into two segments, $[0, \phi_c]$ and $[\phi_c, 1]$, and separately formulate boundary conditions at the ends of these two segments.

The flux through the left boundary $\phi = 0$ of the segment $[0, \phi_c]$ is given by the number of enzymes per unit time that bind a substrate and thus start their cycles:

$$\left[\upsilon\tilde{n} - \sigma \frac{\partial \tilde{n}}{\partial \phi}\right]_{\phi=0} = \alpha s n \tag{15}$$

At point $\phi = \phi_c$ inside the cycle, a product molecule is irreversibly released (which is quickly transformed into the substrate) and the enzyme-substrate complex disappears. Since this occurs with any enzyme when it reaches the state $\phi = \phi_c$, an absorbing boundary condition should be placed at the right end of the segment $[0, \phi_c]$; i.e., we have

$$\tilde{n}|_{\phi=\phi_c} = 0 \tag{16}$$

The segment $[\phi_c, 1]$ corresponds to enzymes that are in the process of conformational relaxation to their free states. The flux through its left boundary $\phi = \phi_c$ should be equal to the flux of enzymes that reach at the considered moment the right boundary of the segment $[0, \phi_c]$. Thus, we obtain

$$\left[\upsilon\tilde{n} - \sigma \frac{\partial \tilde{n}}{\partial \phi}\right]_{\phi=\phi_c+0} = \sigma \frac{\partial \tilde{n}}{\partial \phi}|_{\phi=\phi_c} \tag{17}$$

Here we have used the notation $\phi = \phi_c + 0$ to indicate that the respective flux should be taken at the left boundary of the segment $[\phi_c, 1]$. Moreover, we have taken into account that the absorbing boundary condition 16 holds on the right boundary of segment $[0, \phi_c]$ and therefore $\tilde{n} = 0$ at $\phi = \phi_c$.

Finally, any enzyme that reaches $\phi = 1$ finishes its cycle and becomes free. Therefore, eq 14 should have an absorbing boundary at the right end $\phi = 1$ of the segment $[\phi_c, 1]$, i.e.

$$\tilde{n}|_{\phi=1} = 0 \tag{18}$$

The mean-field evolution equation for the mean number n of free enzymes is

$$\frac{\mathrm{d}n}{\mathrm{d}t} = -\alpha s n + \left[\upsilon\tilde{n} - \sigma \frac{\partial \tilde{n}}{\partial \phi}\right]_{\phi=1} \tag{19}$$

The first term on the right-hand side of this equation takes into account that the number n of free enzymes decreases when they bind a substrate molecule. The second term describes the increase of n through enzymes finishing their cycles and returning to the free state.

Finally, the mean-field evolution equation for the mean number s of substrate molecules in the reaction volume is

$$\frac{ds}{dt} = -\alpha s n + \left[\upsilon \tilde{n} - \sigma \frac{\partial \tilde{n}}{\partial \phi}\right]_{\phi=\phi_c} - \gamma s + \zeta \qquad (20)$$

The first term on the right side describes the decrease in the number of substrate molecules by binding to free enzymes; the second term takes into account the release of new substrate molecules by enzymes at point $\phi = \phi_c$ inside the cycle. The third and fourth terms describe the decay and supply of substrate molecules.

Note that the combination

$$N = n(t) + \int_0^1 \tilde{n}(\phi,t)\, d\phi \qquad (21)$$

is conserved since it represents the total number of enzyme molecules in the system, given by the sum of enzymes in the free state plus enzymes inside the catalytic cycle.

Equations 14−21 constitute the mean-field description of the considered reaction. These equations are formulated by neglecting fluctuations in the numbers of substrate molecules and enzyme molecules in different cycle states, i.e., by replacing the respective exact fluctuating variables by their time-dependent ensemble averages. The effects of intramolecular noise are however taken into account in the equations as leading to an effective diffusion along the reaction coordinate. Below we numerically integrate these equations and compare their predictions with the behavior described by the full stochastic model.

Figure 6a displays the time dependence of the substrate (solid line) and free enzyme (dashed line) concentrations in the mean-field approximation (eqs 14−21) under the same reaction parameters as in Figure 3a. We see that rapid oscillations with period $T \approx \tau_0$ are observed at $\phi_c = 0.2$. The comparison with the respective stochastic simulation in Figures 3a and 6a reveals good agreement: both the oscillation frequency and the amplitude of oscillations are equal in both approaches (though, as should have been expected, fluctuations are absent in the mean-field description).

If we take $\phi_c = 0.55$, spiking with period $T \approx 0.5\tau_0$ is found at low intensities of intramolecular noise in the mean-field description (Figure 6b, $\xi = 0.02$) in good agreement with the result of the respective stochastic simulation (Figure 3b). The self-sustained oscillations disappear at a higher statistical dispersion ξ of the turnover time. Figure 6c displays the time evolution in the concentration of substrate and free enzymes at $\xi = 0.05$ after a small perturbation. The system shows damped oscillations with period $T \approx 0.5\tau_0$ relaxing to a stationary level. Random fluctuations around the same mean level are found in the stochastic model at this value of ξ (cf. Figure 3c).

Further increase in the dispersion ξ of turnover times leads to a change in the mean-field behavior. The oscillations remain damped, but their period changes to $T \approx \tau_0$ (Figure 6d, $\xi = 0.14$). Moreover, we can notice that a perturbation of the same magnitude as in Figure 6c now induces damped oscillations with a much higher initial amplitude. The stochastic model shows persistent noisy oscillations with period $T \approx \tau_0$ at $\xi = 0.14$ (cf. Figure 3d). On the basis of our analysis of the mean-field approximation, they can be interpreted as damped oscillations of period $T \approx \tau_0$ that are persistently induced by the internal noise of the reactive system.

5. Bifurcation Diagram

In the mean-field approximation the onset of spiking corresponds to a bifurcation of the steady state (the fixed point) of eqs 14−21. This Hopf bifurcation transforms the stable fixed point into a stable limit cycle. Thus, by analyzing the stability of this state with respect to small perturbations, boundaries of spiking regimes in the parameter space can be determined.

The steady state is given by a stationary solution of the diffusion eq 14 with boundary conditions 15−18 and of eqs 19 and 20. The mean number s_0 of substrate molecules in the steady state is

$$s_0 = \zeta/\gamma \qquad (22)$$

The mean number n_0 of free enzymes in this steady state is

$$n_0 = \frac{N}{1 + \frac{\alpha s_0}{\upsilon}\left\{1 - \frac{2\sigma}{\upsilon}\left[1 - \exp\left(-\frac{\upsilon\phi_c}{\sigma}\right) - \exp\left(-\frac{\upsilon(1-\phi_c)}{\sigma}\right)\right]\right\}} \qquad (23)$$

The stability of this stationary solution can be analyzed by investigating the evolution of small perturbations, introduced as $s(t) = s_0 + \delta s(t)$, $n(t) = n_0 + \delta n(t)$, and $\tilde{n}(\phi,t) = \tilde{n}_0(\phi) + \delta\tilde{n}(\phi,t)$. Linearization of the evolution equations yields

$$\frac{d\delta n}{dt} = -\alpha s_0 \delta n - \alpha n_0 \delta s + \left[\upsilon \delta\tilde{n} - \sigma \frac{\partial \delta\tilde{n}}{\partial \phi}\right]_{\phi=1} \qquad (24)$$

$$\frac{d\delta s}{dt} = -\alpha s_0 \delta n - \alpha n_0 \delta s + \left[\upsilon \delta\tilde{n} - \sigma \frac{\partial \delta\tilde{n}}{\partial \phi}\right]_{\phi=\phi_c} - \gamma \delta s \qquad (25)$$

$$\frac{\partial \delta\tilde{n}}{\partial t} = -\upsilon \frac{\partial \delta\tilde{n}}{\partial \phi} + \sigma \frac{\partial^2 \delta\tilde{n}}{\partial \phi^2} \qquad (26)$$

Their solutions must satisfy linearized boundary conditions:

$$\left[\upsilon \delta\tilde{n} - \sigma \frac{\partial \delta\tilde{n}}{\partial \phi}\right]_{\phi=0} = \alpha s_0 \delta n + \alpha n_0 \delta s \qquad (27)$$

$$\left[\upsilon \delta\tilde{n} - \sigma \frac{\partial \delta\tilde{n}}{\partial \phi}\right]_{\phi=\phi_c+0} = \sigma \frac{\partial \delta\tilde{n}}{\partial \phi}\Big|_{\phi=\phi_c} \qquad (28)$$

$$[\delta\tilde{n}]_{\phi=\phi_c} = [\delta\tilde{n}]_{\phi=1} = 0 \qquad (29)$$

Finding a solution of eqs 24−29 can be simplified if we restrict our analysis to small values of the diffusion constant σ. Moreover, we take into account that the expected characteristic time scale of the first unstable oscillatory mode is on the order of τ_0. For such processes, the influence of the absorbing boundary conditions 29 extends only over narrow intervals of width $(\sigma\tau_0)^{1/2}$ to the left from the respective boundaries. Outside of such narrow intervals, the diffusion drift eq 26 has the same solution as in the absence of these boundaries.

Looking at eqs 24 and 25, we notice that fluxes $J = \upsilon\delta\tilde{n} - \sigma(\partial\delta\tilde{n}/\partial\phi)$ at ϕ_c and $\phi = 1$ are needed. We would introduce only a small error if we evaluate these fluxes not at points $\phi = \phi_c$ and $\phi = 1$, but at the locations shifted by a distance of $(\sigma\tau_0)^{1/2}$ slightly to the left from these points. To determine the fluxes J, we can use then, however, the solutions of a simplified problem where the boundaries at $\phi = \phi_c$ and $\phi = 1$ are eliminated. In this case, the diffusion drift eq 26 is formally defined on the interval from $\phi = 0$ to infinity and only the boundary condition 27 is imposed. This boundary condition specifies the flux that enters the considered interval.

The solutions of the linear differential eqs 24−26 with the boundary condition 27 can be sought in the form $\delta\tilde{n}(\phi,t) = A \exp(\lambda t - k\phi)$, $\delta s(t) = B \exp(\lambda t)$, and $\delta n(t) = C \exp(\lambda t)$. Substituting these expressions into the differential equations,

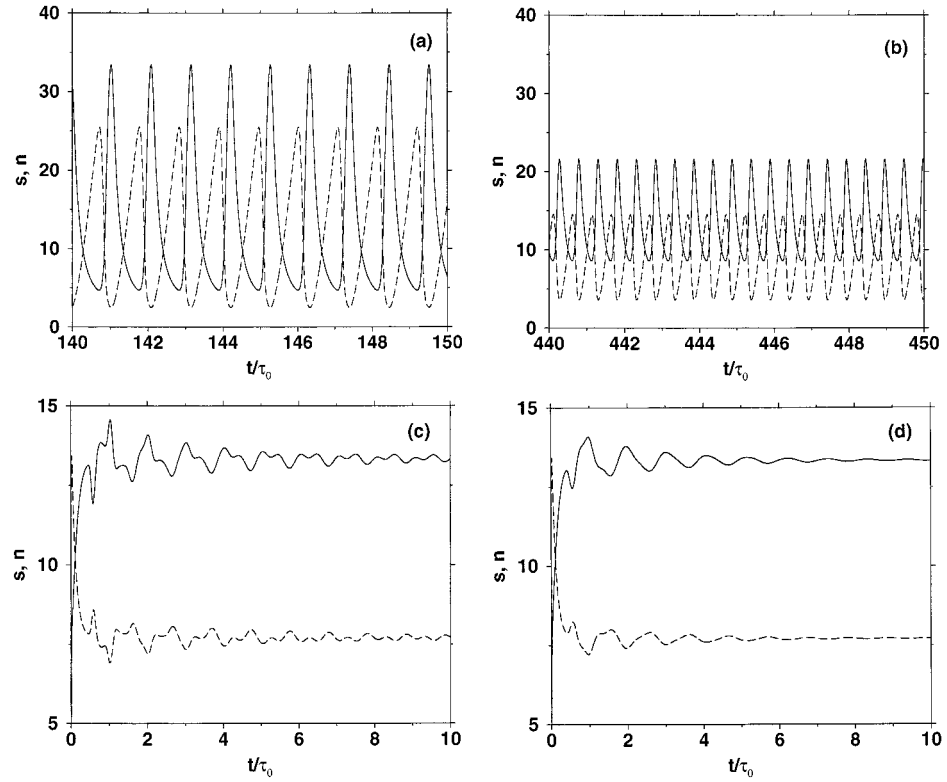

Figure 6. Time dependence of the number of substrate molecules (solid line) and free enzymes (dashed line) obtained by numerical integration of the mean-field model. The parameters in parts a−d are the same as in the respective parts a−d of Figure 2.

we obtain the dispersion relation

$$k = -\frac{\nu}{2\sigma} + \left(\frac{\nu^2}{4\sigma} + \frac{\lambda}{\sigma}\right)^{1/2} \tag{30}$$

and a system of linear homogeneous equations

$$\hat{\mathbf{D}}\begin{pmatrix} A \\ B \\ C \end{pmatrix} = \lambda \begin{pmatrix} A \\ B \\ C \end{pmatrix} \tag{31}$$

with the coefficient matrix

$$\hat{\mathbf{D}} = \begin{pmatrix} \nu - \sigma k(\lambda) & -\alpha n_0 & -\alpha s_0 \\ (\sigma k(\lambda) - \nu)\, \mathrm{e}^{k(\lambda)} & \lambda + \gamma + \alpha n_0 & \alpha s_0 \\ (\sigma k(\lambda) - \nu)\, \mathrm{e}^{k(\lambda)\phi_c} & \alpha n_0 & \lambda + \alpha s \end{pmatrix} \tag{32}$$

The solvability condition of the system is given by the characteristic equation

$$\det(\hat{\mathbf{D}} - \lambda \mathbf{I}) = 0 \tag{33}$$

The roots of this quasi-polynomial are generally an infinite set of complex numbers $\lambda_j = \Gamma_j + i\omega_j$. If for a chosen set of parameters the real parts of all eigenvalues λ_j are $\Gamma_j < 0$, the steady state is stable. If for at least one eigenvalue $\Gamma_j > 0$, the steady state is unstable with respect to growth of oscillations with frequency ω_j and period $T_j = 2\pi/\omega_j$. The instability boundary is thus determined by the condition that $\Gamma_i = 0$ for at least one eigenmode j.

To numerically determine the critical parameter values at which a bifurcation is found, we first take $\Gamma_j = 0$ at $j = 1$ and seek the absolute minimum of

$$|\det(\hat{\mathbf{D}} - \lambda \mathbf{I})|$$

in the vicinity of $\omega_1 \approx 2\pi\tau_0^{-1}$ under varying the respective bifurcation parameter. Next we apply the same procedure for $j = 2$, and so on.

Figure 7a displays the bifurcation boundaries in the parameter plane (ϕ_c, α) obtained by such a numerical solution of eq 33. The real part of λ vanishes on the bifurcation boundaries, whereas the imaginary part is finite. This imaginary part determines the frequency of oscillations that develop when the steady state loses its stability. The steady state is unstable and spiking with periods $T_1 \approx \tau_0$ and $T_2 \approx 0.5\tau_0$ develops inside the regions whose boundaries are indicated by the solid and dashed lines, respectively. Thus, if we keep ϕ_c constant and increase the binding probability rate constant α, the steady state becomes unstable and oscillations develop when the lower boundary is crossed. However, if we further increase α and cross the upper boundary, the oscillations disappear and the stable steady state is re-established. Hence, oscillations are expected only in a certain window of the parameter α.

Figure 7b shows the analogous bifurcation boundaries in the parameter plane (ξ, α). The solid line in Figure 7b is the boundary of the instability region at $\phi_c = 0.2$ inside which the system oscillates with period $T_1 \approx \tau_0$. The dashed line limits the instability region at $\phi_c = 0.55$ inside which oscillations with shorter period $T_2 \approx 0.5\tau_0$ take place.

The bifurcation diagram in the parameter plane (γ, α) is displayed in Figure 7c. When the decay rate γ of the substrate is below $\gamma = 7\tau_0^{-1}$, the steady state of the system remains stable. In the range $7\tau_0^{-1} \le \gamma \le 15.5\tau_0^{-1}$ the system may show oscillations with period $T_1 \approx \tau_0$. Above $\gamma = 15.5\tau_0^{-1}$, oscillations with period $T_1 \approx \tau_0$ or $T_2 \approx 0.5\tau_0$ can develop, depending on the parameter ϕ_c.

In the last bifurcation diagram (Figure 7d) the dependence of the synchronization threshold on the rate ζ of the substrate supply is shown. Again the solid line determines the instability boundary for spiking with $T_1 \approx \tau_0$ at $\phi_c = 0.2$ and the dashed line for $T_2 \approx 0.5\tau_0$ at $\phi_c = 0.55$. Note that the region of

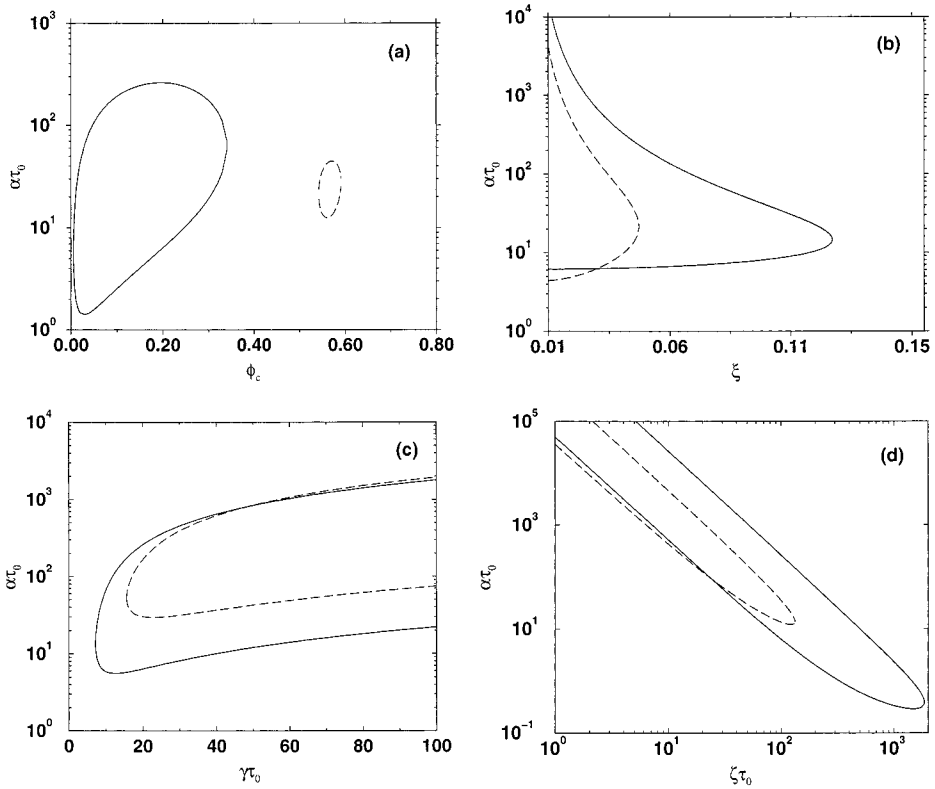

Figure 7. Bifurcation diagrams (a) in the parameter plane (α, ϕ_c), (b) in the parameter plane (α, ξ), (c) in the parameter plane (α, γ), and (d) in the parameter plane (α, ζ), obtained by the stability analysis of the fixed point in the mean-field approximation for two different values of ω. The solid curves are for $\omega \approx 2\pi\tau_0^{-1}$ and the dashed curves are for $\omega \approx 4\pi\tau_0^{-1}$. When the parameters are fixed, they take values $\gamma = 20\tau_0^{-1}$, $\zeta = 100\tau_0^{-1}$, $\xi = 0.04$. In parts b, c and d the solid curves correspond to $\phi_c = 0.2$ and the dashed curves correspond to $\phi_c = 0.55$.

oscillations with period $T_2 \approx 0.5\tau_0$ extends over 3 orders of magnitude of the supply rate ζ, and for oscillations with period $T_1 \approx \tau_0$ even over 4 orders of magnitude of this parameter. At small values of ζ the oscillations are found at high substrate binding rate constants α.

6. Conclusions

We have presented a theoretical investigation of coherent intramolecular dynamics in a model reaction chain including a reaction step catalyzed by an enzyme. The analysis was performed under the assumption of a small spatial reaction volume, where the characteristic diffusive transport and mixing times are much shorter than the mean turnover time of the enzymes. In contrast to the previous publications, where allosterically activated and inhibited enzyme reactions[20,21] were investigated, the enzymes in the present reaction model did not have any regulatory properties. Despite this, the synchronization of enzymic molecular turnover cycles and rapid spiking in the product concentration were found in this system.

This conclusion, obtained by direct numerical simulations of the stochastic reaction model, is confirmed by the analysis of the mean-field approximation that was constructed for the considered reaction. This has allowed us to derive the bifurcation diagram and analytically determine the regions in the parameter space of the model where coherent collective enzyme dynamics is expected.

We have found that, depending on the microscopic properties of an individual molecular turnover cycle, the same reaction chain can form two coherently operating enzymic groups, whose phases are shifted by half of the period, or show complete synchronization. This is similar to the behavior that was previously noticed for the allosterically activated reaction.[20] A new effect, representing a transition from the coherent two-group regime to synchronous oscillations of the entire enzymic ensemble, was discovered for the considered reaction under an increase of the intensity of intramolecular noises. The synchronization of turnover cycles and coherent intramolecular dynamics were found in the present study even at relatively high intensities of intramolecular fluctuations, such that the statistical dispersion of turnover times could reach $\pm 20\%$.

Thus, the results of our investigations suggest that the spontaneous emergence of coherent intramolecular dynamics is a robust phenomenon that can be expected for both allosteric and nonallosteric enzymes in the reactions proceeding in biologically relevant microvolumes.

Acknowledgment. We acknowledge financial support from "Peter und Traudl Engelhorn Stiftung zur Förderung der Biotechnologie und Gentechnik" (Germany).

7. Appendix

In this Appendix we present the algorithms used in our numerical simulations of the stochastic model of reactions 1 and 10.

Time is divided into equal small steps Δt. For each enzyme i the binary variable u_i is defined, so that $u_i(t) = 0$ if this enzyme is in the free state at time t and $u_i(t) = 1$ if enzyme i is inside its turnover cycle at time t. The stochastic differential eq 4 is replaced by the finite difference equation

$$\phi_i(t+\Delta t) = \phi_i(t) + v\Delta t + \sigma\varsigma_i(\Delta t)^{1/2} \qquad (34)$$

where ς_i are independent Gaussian random numbers, such that

$$\langle \varsigma_i \varsigma_j \rangle = 2\delta_{ij}$$

The cycle starts with $\phi_i = 0$ at the moment when the enzyme binds the substrate molecule, i.e., when the variable u_i changes from 0 to 1. If after the cycle initiation the right part of eq 24 becomes smaller than zero, it is replaced by $v\Delta t$. The cycle is finished and the enzyme returns to its free state $u_i = 0$ at the moment $t + \Delta t$, such that $\phi_i(t) < 1$ but $\phi_i(t+\Delta t) \geq 1$. Once the product is released by enzyme i and its phase is $\phi_i > \phi_c$, this phase is not allowed to later become smaller than ϕ_c. If by chance the right side of eq 24 becomes smaller than ϕ_c, it is replaced in our algorithm by $\phi_c + v\Delta t$.

The updating algorithm for the binary state variables $u_i(t)$ is

$$u_i(t+\Delta t) = \begin{cases} 1, \text{ if } u_i(t) = 0, \text{ with probability } \alpha s(t)\,\Delta t \\ 0, \text{ if } u_i(t) = 0, \text{ with probability } 1 - \alpha s(t)\,\Delta t \\ 0, \text{ if } u_i(t) = 1, \text{ and } \phi_i(t+\Delta t) \geq 1 \\ 1, \text{ if } u_i(t) = 1, \text{ and } \phi_i(t+\Delta t) < 1 \end{cases} \quad (35)$$

where α is the substrate binding rate constant and $s(t)$ is the number of substrate molecules.

The number m of product molecules in the model of reaction 1 is updated according to the algorithm

$$m(t+\Delta t) = m(t) + \sum_{i=1}^{N} u_i(t)\,\Theta\,(\phi_i(t+\Delta t) - \phi_c)\,\Theta\,(\phi_c - \phi_i(t)) - \sum_{j=1}^{m} \chi_j - \sum_{k=1}^{N} \rho_k \quad (36)$$

where χ_j and ρ_k are independent binary random numbers taking values 1 and 0 with probabilities $\gamma_1\Delta t$, $1 - \gamma_1\Delta t$ and $\kappa\Delta t$, $1 - \kappa\Delta t$, respectively. The step function $\Theta(x)$ is defined as $\Theta(x) = 1$ if $x \geq 0$ and $\Theta(x) = 0$ if $x < 0$. The second term on the right side of eq 36 takes into account that a new product molecule is released and therefore m is increased by 1, whenever one of the enzymes goes through the point ϕ_c. The third term describes the stochastic decay of products: each of the m products can die with the small probability $\gamma\Delta t$ within time interval Δt, thus decreasing the number m. The last term in this equation takes into account that the number M of product molecules decreases through conversion into substrate molecules with the probability $\kappa\Delta t$.

The number of free substrate molecules in the model of reaction 1 is updated as

$$s(t+\Delta t) = s(t) - \sum_{i=1}^{N} (1 - u_i(t))u_i(t+\Delta t) - \sum_{j=1}^{s} \psi_j + \sum_{k=1}^{m} \rho_k + Z \quad (37)$$

The second term on the right side describes the decrease of substrate molecules when they bind to an enzyme. The third term takes into account the decay of substrate at rate γ. Here ψ_j is a binary random number taking values 1 and 0 with probabilities $\gamma\Delta t$ and $1 - \gamma\Delta t$. The fourth term takes into account the increase of substrate molecules by converted product molecules. The last term describes the supply of substrate molecules. Here Z is a random number that can take positive integer values or zero. It obeys the Poisson distribution with the mean value $\zeta\Delta t$.

In the model of reaction 10 eqs 36 and 37 are replaced by the single equation where the random number ψ_j is defined as

$$s(t+\Delta t) = s(t) + \sum_{i=1}^{N} u_i(t)\,\Theta\,(\phi_i(t+\Delta t) - \phi_c)\,\Theta\,(\phi_c - \phi_i(t)) - \sum_{j=1}^{s} \psi_j - \sum_{i=1}^{N} (1 - u_i(t))u_i(t + \Delta t) + Z \quad (38)$$

in eq 37. The second term takes into account the release of a product molecule, instantaneously converting to the substrate molecule, by enzymes passing through the phase point ϕ_c. The third term describes the decay of substrate. The fourth term takes into account binding of substrate molecules by free enzymes. The last term describes the supply of substrate molecules.

References and Notes

(1) Blumenfeld, L. A.; Tikhonov, A. N. *Biophysical Thermodynamics of Intracellular Processes*; Springer: Berlin, 1994.
(2) Subbiah, S. *Protein Motions*; Springer: Berlin, 1996.
(3) Petsko, G. A. *Nature* **1994**, *371*, 740.
(4) Schlichting, I.; Berendzen, J.; Phillips, G. N.; Sweet, R. M. *Nature* **1994**, *371*, 808.
(5) Eigen, M.; Rigler, R. *Proc. Natl. Acad. Sci. U.S.A.* **1994**, *91*, 5740.
(6) Weiss, S. *Science* **1999**, *283*, 5408.
(7) Lu, H. P.; Luying, X.; Xie, X. S. *Science* **1998**, *282*, 1877.
(8) Ishijima, A.; Kojima, H.; Funatsu, T.; Tokunaga, M.; Higuchi, H.; Tanaka, M.; Yanagida, T. *Cell* **1998**, *92*, 161.
(9) Hess, B.; Mikhailov, A. S. *Science* **1994**, *264*, 223.
(10) Hess, B.; Mikhailov, A. S. *J. Theor. Biol.* **1995**, *176*, 181.
(11) Alberts, B. *Cell* **1998**, *92*, 291.
(12) Service, R. F. *Science* **1999**, *284*, 80.
(13) Chiu, D. T.; Clyde, F. W.; Ryttsen, F.; et al. *Science* **1999**, *283*, 1892.
(14) Gruler, H.; Müller-Enoch, D. *Eur. Biophys. J.* **1991**, *19*, 217.
(15) Häberle, W.; Gruler, H.; Dutkowski, Ph.; Müller-Enoch, D. *Z. Naturforsch.* **1990**, *45c*, 237.
(16) Schienbein, M.; Gruler, H. *Phys. Rev. E* **1997**, *56*, 7116.
(17) Derenyi, I.; Astumian D. R. *Phys. Rev. Lett.* **1998**, *80*, 4602.
(18) Hess, B.; Mikhailov, A. S. *Biophys. Chem.* **1996**, *58*, 365.
(19) Mikhailov, A. S.; Hess, B. *J. Phys. Chem.* **1996**, *100*, 19059.
(20) P.Stange, Mikhailov, A. S.; Hess, B. *J. Phys. Chem. B* **1998**, *102*, 6273.
(21) Stange, P.; Mikhailov, A. S.; Hess, B. *J. Phys. Chem. B* **1999**, *103*, 6111.
(22) Stryer, L. *Biochemistry*, 3rd ed.; Freeman: New York, 1995.
(23) Hess, B.; Mikhailov, A. S. *Ber. Bunsen-Ges. Phys. Chem.* **1994**, *98*, 1198.